1521-0111/12/8102-198–209$25.00
MOLECULAR PHARMACOLOGY
Copyright © 2012 The American Society for Pharmacology and Experimental Therapeutics
Mol Pharmacol 81:198–209, 2012

Vol. 81, No. 2
75135/3742832

Molecular Determinants of Pentamidine-Induced hERG Trafficking Inhibition[S]

Adrienne T. Dennis, Lu Wang, Hanlin Wan, Drew Nassal, Isabelle Deschenes, and Eckhard Ficker

Rammelkamp Center for Education and Research, MetroHealth Campus (A.T.D., L.W., H.W., D.N., I.D., E.F.) and Department of Physiology and Biophysics (D.N., I.D.), Case Western Reserve University, Cleveland, Ohio

Received August 3, 2011; accepted November 1, 2011

ABSTRACT

Pentamidine is an antiprotozoal compound that clinically causes acquired long QT syndrome (acLQTS), which is associated with prolonged QT intervals, tachycardias, and sudden cardiac arrest. Pentamidine delays terminal repolarization in human heart by acutely blocking cardiac inward rectifier currents. At the same time, pentamidine reduces surface expression of the cardiac potassium channel I_{Kr}/human ether à-go-go-related gene (hERG). This is unusual in that acLQTS is caused most often by direct block of the cardiac potassium current I_{Kr}/hERG. The present study was designed to provide a more complete picture of how hERG surface expression is disrupted by pentamidine at the cellular and molecular levels. Using biochemical and electrophysiological methods, we found that pentamidine exclusively inhibits hERG export from the endoplasmic reticulum to the cell surface in a heterologous expression system as well as in cardiomyocytes. hERG trafficking inhibition could be rescued in the presence of the pharmacological chaperone astemizole. We used rescue experiments in combination with an extensive mutational analysis to locate an interaction site for pentamidine at phenylalanine 656, a crucial residue in the canonical drug binding site of terminally folded hERG. Our data suggest that pentamidine binding to a folding intermediate of hERG arrests channel maturation in a conformational state that cannot be exported from the endoplasmic reticulum. We propose that pentamidine is the founding member of a novel pharmacological entity whose members act as small molecule antichaperones.

Introduction

Pentamidine is an antiprotozoal compound, used in the treatment of trypanosomiasis, leishmaniasis, and *Pneumocystis carinii* pneumonia, that causes drug-induced or acquired long QT syndrome (acLQTS) in clinical use (Sands et al., 1985; Wharton et al., 1987; Bibler et al., 1988; Girgis et al., 1997; Nacher et al., 2001; Burchmore et al., 2002). acLQTS produces electrocardiographic abnormalities that have been associated with syncope, torsades de pointes arrhythmias, and sudden cardiac death (Kannankeril et al., 2010) and are most often caused by direct block of the cardiac potassium current I_{Kr}/hERG, which is crucial for terminal repolarization in human heart (Sanguinetti and Tristani-Firouzi, 2006). Because hERG block constitutes an adverse side effect of therapeutic compounds as well as a significant hurdle in the development of novel drug compounds, several preclinical assays have been developed for early detection, including binding assays and the so-called hERG assay, which consists of patch-clamp measurements performed on cloned hERG channels (Thomsen et al., 2006; Pollard et al., 2010). It is noteworthy that a number of therapeutic compounds are undetected in conventional assays targeting direct hERG block (Dennis et al., 2007; van der Heyden et al., 2008). For example, we have shown that arsenic trioxide, which is used in the treatment of leukemia (Ficker et al., 2004), reduces the number of hERG channels at the cell surface by inhibiting the maturation of hERG channels in the endoplasmic reticulum (ER) and preventing export from the ER. At the same time, arsenic trioxide increases cardiac

This work was supported in part by the National Institutes of Health National Heart, Lung, and Blood Institute [Grants T32-HL105338, 1R01-HL096962].

Article, publication date, and citation information can be found at http://molpharm.aspetjournals.org.

http://dx.doi.org/10.1124/mol.111.075135.

[S] The online version of this article (available at http://molpharm.aspetjournals.org) contains supplemental material.

ABBREVIATIONS: acLQTS, acquired long QT syndrome; hERG, human ether à-go-go-related gene; ER, endoplasmic reticulum; HEK, human embryonic kidney; WT, wild type; DMEM, Dulbecco's modified Eagle's medium; bEAG, bovine ether-à-go-go; NRVM, Neonatal rat ventricular myocyte; PAGE, polyacrylamide gel electrophoresis; fg, fully glycosylated 150-kDa cell surface form of hERG; cg, core-glycosylated 135-kDa ER-resident form of hERG; I_{Kr}, rapidly activating delayed rectifier K current; Hsp90, 90-kDa heat shock protein; PBS, phosphate-buffered saline; HA, hemagglutinin; MK-499, (+)-*N*-[1′-(6-cyano-1,2,3,4-tetrahydro-2(*R*)-naphthalenyl)-3,4-dihydro-4(*R*)-hydroxyspiro(2*H*-1-benzopyran-2,4′-piperidin)-6-yl]methanesulfonamide] monohydrochloride.

calcium currents via oxidative inactivation of the lipid phosphatase known as "phosphatase and tensin homolog on chromosome 10" (Wan et al., 2011). Both mechanisms converge to create cardiac repolarization abnormalities that are reflected in a high incidence of adverse cardiac events during therapy (Ohnishi et al., 2000, 2002; Barbey et al., 2003). Likewise, a large number of direct hERG blockers provide a double hit on cardiac repolarization in that they combine conventional hERG block with unconventional hERG trafficking inhibition (Wible et al., 2005; Rajamani et al., 2006; Takemasa et al., 2008; Obers et al., 2010; Staudacher et al., 2011). Unfortunately, few compounds that cause acLQTS by unconventional mechanisms have been fully characterized at the cellular and molecular level.

Dicationic pentamidine is another example of a therapeutic compound that has been associated with a high incidence of cardiac arrhythmias because of a combination of unconventional mechanisms: 1) reduced hERG surface expression and 2) acute block of cardiac inward rectifier channels, which destabilizes the cardiac membrane potential late during repolarization and under resting conditions (Cordes et al., 2005; Ficker et al., 2005; Kuryshev et al., 2005; de Boer et al., 2010). Although a mechanistic model for acute block of cardiac inward rectifier channels by pentamidine has been developed (de Boer et al., 2010), the precise mechanisms by which pentamidine interferes with hERG surface expression are unknown. Currently, it is known only that the fully glycosylated cell surface form of hERG together with the corresponding membrane currents disappear after long-term incubation with pentamidine (Kuryshev et al., 2005). It is noteworthy that pentamidine does not directly block hERG in the therapeutic concentration range (Cordes et al., 2005).

We focus here on how hERG surface expression is disrupted by pentamidine at the cellular and molecular level. We find that pentamidine exclusively inhibits export of hERG from the ER. We show for the first time that pentamidine arrests hERG maturation in a nonexportable conformation via binding to a critical amino acid residue, Phe656, which contributes to the well characterized canonical drug binding site in the conduction pathway of terminally folded hERG. We propose that pentamidine may inhibit hERG trafficking by acting as a novel pharmacological entity known as a small-molecule "antichaperone."

Materials and Methods

Cell Culture. Human embryonic kidney (HEK) 293 cells stably expressing hERG WT (HEK/hERG WT), were maintained at 37°C, 5% CO_2 in DMEM supplemented with 10% fetal bovine serum, L-glutamine, penicillin/streptomycin (complete DMEM), and G418. Point mutations of hERG were engineered either by overlap extension polymerase chain reaction or by using the QuikChange site-directed mutagenesis kit (Stratagene, La Jolla, CA). All mutant constructs were verified by sequencing. Several different mutant hERG channel cDNAs were gifts from M. Sanguinetti (University of Utah, Salt Lake City, UT) and S. Zhang (Queen's University, Kingston, ON, Canada). Mutant hERG as well as bEAG WT (bovine ether-à-go-go) were transiently expressed in HEK293 cells using FuGENE 6 transfection reagent (Roche Diagnostics, Indianapolis, IN), and compared with transiently transfected hERG WT.

HL-1 cardiomyocytes were maintained as described by Claycomb et al. (1998). In brief, HL-1 cells were plated on culture dishes coated with gelatin and fibronectin and maintained at 37°C in an atmosphere of 95% humidified air and 5% CO_2 in Claycomb Medium (Sigma-Aldrich, St. Louis, MO) supplemented with 10% fetal bovine serum, 2 mM L-glutamine, 0.1 mM norepinephrine (Sigma-Aldrich), 100 U/ml penicillin, and 100 μg/ml streptomycin. The medium was changed approximately every 24 to 48 h. When confluent, cells were dissociated using trypsin/EDTA (Invitrogen, Carlsbad, CA) and resuspended in complete Claycomb Medium at a density of 25×10^6 cells/60-mm dish for Western blotting and at a density of 25×10^3 cells/gelatin-fibronectin–coated coverslip for electrophysiological recordings.

Neonatal rat ventricular myocytes (NRVM) were isolated from dissected hearts of 1- to 2-day-old rat pups as described previously. All procedures conformed to institutional guidelines for the care and use of animals in research. In brief, hearts were minced in Hanks' balanced salt solution and tissue fragments were digested overnight with trypsin at 4°C. Trypsinized tissue fragments were treated repeatedly for short periods with collagenase at 37°C followed by trituration. Dissociated cells were filtered, collected via centrifugation, and preplated for 2 h to remove fibroblasts. Supernatants from "preplating" dishes were replated in DMEM/5% fetal bovine serum/penicillin/streptomycin at a density of 4×10^6 NRVMs/60-mm culture dish. NRVM cultures were maintained at 37°C, 5% CO_2 with bromodeoxyuridine added to suppress fibroblast growth. For electrophysiological studies, NRVMs were grown on collagen-coated glass coverslips. Experiments were typically performed 2 to 4 days after initial plating.

Pentamidine (Sigma-Aldrich) was added to cell cultures for either 0.5 to 6 h (short-term) or 16 to 24 h (overnight) before Western blot analysis or current recordings. Pentamidine stock solutions were prepared in water. A stock solution of astemizole was prepared in dimethyl sulfoxide. Final dimethyl sulfoxide concentrations of drug-containing solutions did not exceed 0.1%.

Cellular Electrophysiology. Current recordings from HEK cells and HL-1 cardiomyocytes were performed using patch pipettes filled with 100 mM potassium aspartate, 20 mM KCl, 2 mM $MgCl_2$, 1 mM $CaCl_2$, 10 mM EGTA, and 10 mM HEPES, pH 7.2. The extracellular recording solution consisted of 140 mM NaCl, 5 mM KCl, 1 mM $MgCl_2$, 1.8 mM $CaCl_2$, 10 mM HEPES, and 10 mM glucose, pH 7.4. Some hERG mutants with ultrafast current inactivation were recorded in the presence of 140 mM KCl as an equimolar substituent for NaCl in the extracellular solution. In NRVMs, hERG/I_{Kr} currents were recorded in isotonic Cs^+-solutions (pipette, 135 mM CsCl, 1 mM $MgCl_2$, 10 mM EGTA, and 10 mM HEPES, pH 7.2; extracellular recording solution: 135 mM CsCl, 1 mM $MgCl_2$, 10 mM HEPES, 10 mM glucose, and 1 μM nisoldipine, pH 7.4; Zhang, 2006). pClamp software and an Axon 200B patch clamp amplifier (Molecular Devices, Sunnyvale, CA) were used for the generation of voltage-clamp protocols and data acquisition. To analyze current densities, membrane capacitance was measured using the analog compensation circuit of the patch clamp amplifier. All current recordings were performed at room temperature (20–22°C).

Western Blot Analysis. A previously described polyclonal anti-hERG antibody, rabbit hERG 519, was used to analyze hERG expression in HEK cells (Ficker et al., 2003). In HL-1 cardiomyocytes and NRVMs, hERG/I_{Kr} expression was analyzed using a polyclonal anti-hERG-GST antibody from Alomone Labs (Jerusalem, Israel). In brief, HEK/hERG cells or cardiomyocytes were solubilized for 1 h at 4°C in lysis buffer containing 150 mM NaCl, 1 mM EDTA, 50 mM Tris, pH 7.5, 1% Triton X-100, and protease inhibitors (Complete protease inhibitor; Roche Diagnostics). Protein concentrations were determined by the bicinchoninic acid method (Thermo Fisher Scientific, Waltham, MA). Proteins were separated on SDS polyacrylamide gels, transferred to polyvinylidene difluoride membranes, and developed using the appropriate anti-hERG antibody, followed by horseradish peroxidase-conjugated secondary antibody and ECL Plus (GE Healthcare, Chalfont St. Giles, Buckinghamshire, UK). For quantitative analysis, signals were captured directly on a Kodak Imager R4000 (Carestream Health, Rochester, NY).

hERG Ubiquitination. In ubiquitination studies, stable HEK/hERG WT cells were transiently transfected with either HA-ubiquitin or His_6-ubiquitin cDNA using FuGENE (Roche Diagnostics). Cells were harvested 2 days after transfection. In experiments with pentamidine, cells were treated overnight on the second day after transfection. Whole-cell lysates were immunoprecipitated with anti-hERG antibody. Immunoprecipitates were analyzed on Western blots using either antibody to hERG or to the HA epitope fused to ubiquitin. Lysates with His_6-ubiquitin were used as negative control.

Sucrose Gradients. HEK/hERG WT cells (pentamidine treated or untreated controls) were lysed in digitonin lysis buffer containing 150 mM NaCl, 10 mM Tris, pH 7.4, 1% digitonin, and protease inhibitors (Complete protease inhibitor; Roche Diagnostics). Soluble material (400–800 μg of total protein) was layered onto 15 to 45% sucrose gradients (150 mM NaCl, 10 mM Tris, pH 7.4, and 0.1% digitonin). Gradients were made using BIOCOMP Gradient Mate (BIOCOMP, Fredericton, NB, Canada) as described previously (Wang et al., 2009). After centrifugation, 275-μl fractions were collected manually from the top of each gradient. Aliquots of individual fractions were concentrated using PAGEprep Protein Clean-Up and Enrichment Kit (Pierce) before loading onto a SDS/PAGE gel for Western blotting.

Pulse-Chase and hERG-Chaperone-Interaction Studies. Pulse-chase and hERG-chaperone-interaction experiments were performed as described previously (Ficker et al., 2003). In brief, HEK/hERG WT cells were starved for 30 min and pulse labeled for 60 min in 100 to 150 μCi/ml [^{35}S]methionine/cysteine-containing medium. Cells were harvested immediately after labeling or after different chase periods in label-free medium. Pentamidine was added for 24 h before labeling. Cells were lysed in a 0.1% Tergitol-type NP-40 buffer in the presence of protease inhibitor. Lysates were immunoprecipitated with anti-hERG antibody (Alomone Labs) and collected with Protein G Dynabeads (Invitrogen). Immunoprecipitated radiolabeled proteins were separated by SDS-PAGE, and analyzed with a Storm PhosphorImager (GE Healthcare). In pulse chase experiments, image densities of fully glycosylated (fg) and core-glycosylated (cg) hERG were normalized to the signal of freshly synthesized, cg-hERG protein isolated immediately after radiolabeling at $t = 0$.

To study hERG-chaperone interactions, HEK/hERG WT cells were labeled and chased in the absence or presence of pentamidine as described above. Immunoprecipitations were performed either with anti-hERG, anti-Hsp/c70, or anti-Hsp90 antibody (Santa Cruz Biotechnology, Santa Cruz, CA), separated by SDS-PAGE, and analyzed with a Storm PhosphorImager (Ficker et al., 2003). HERG-chaperone interactions were studied after treatment of labeled HEK/hERG cells with the chemical cross-linker dithiobis(succinimidyl propionate) (Thermo Fisher Scientific). Cross-linking was reversed by boiling in β-mercaptoethanol/SDS buffer. Image densities of cg-hERG were normalized to densities measured immediately after labeling to assess time-dependent changes in hERG-chaperone interactions as a function of time and drug exposure.

Immunocytochemistry. HEK-hERG cells were grown overnight on poly-lysine–coated glass coverslips under control conditions or in the presence of 30 μM pentamidine. After incubation, cells were washed with PBS and fixed in ice-cold 4% formaldehyde/PBS for 30 min. After fixation, cells were permeabilized with 0.1% Triton X-100 and blocked in 5% goat serum/PBS for 30 to 60 min at room temperature. For double labeling, permeabilized cells were incubated overnight at 4°C with rabbit anti-hERG GST antibody and mouse anti-KDEL antibody (Ficker et al., 2003). The tetrapeptide KDEL, located at the carboxyl-terminal sequences of luminal ER proteins, is a common motif expressed in the ER that is well suited to be a compartment marker. For staining, cells were incubated for 2 h at room temperature with secondary anti-rabbit fluorescein isothiocyanate (The Jackson Laboratory, Bar Harbor, ME) and anti-mouse Rhodamine RedX antibody (The Jackson Laboratory). Coverslips were mounted with Vectashield (Vector Laboratories, Burlingame, CA) and imaged using a laser-scanning confocal microscope (TCS SP2; Leica Microsystems, Wetzlar, Germany).

Data Analysis. Data are expressed as mean ± S.E. of n experiments or cells studied. Differences between means were tested using either a two-tailed Student's t test or single-factor analysis of variance followed by a two-tailed Dunnett's test to determine whether multiple treatment groups were significantly different from control. P values < 0.05 were considered statistically significant.

Results

Pentamidine Inhibits hERG Forward Trafficking. We and others have previously reported that pentamidine reduces cell surface expression of hERG within 24 h in a concentration-dependent manner (Cordes et al., 2005; Kuryshev et al., 2005). However, whether pentamidine decreases hERG stability directly at the cell surface or, alternatively, inhibits hERG forward trafficking from the ER remained unresolved. To determine hERG surface stability as a function of drug exposure, we studied the time course of pentamidine effects by incubating HEK/hERG cells for 0.5 to 24 h with 30 μM pentamidine. When analyzed on Western blots (Fig. 1A), we found that the fully glycosylated 155-kDa cell surface form of hERG (fg-hERG) decayed in the presence of pentamidine with a half-life of 10.5 h, which compared well with a half-life of approximately 11 h determined for fg-hERG under control conditions in pulse-chase experiments (Ficker et al., 2003). In marked contrast, fg-hERG decayed much faster, with a half-life of 2.4 h on incubation with 0 $[K^+]_{ex}$, which is known to increase endocytic uptake of hERG channels from the cell surface (Fig. 1B; Guo et al., 2009). The slow reduction of fg-hERG on Western blots was also reflected in electrophysiological recordings, where we measured hERG current densities of 67.1 ± 10.2 pA/pF ($n = 10$) under control conditions, of 69.6 ± 20.8 pA/pF ($n = 7$) after 6-h exposure to pentamidine, and of 4.9 ± 1.7 pA/pF after 24-h exposure to pentamidine ($n = 6$; Fig. 1, C and D). Furthermore, expression of the core-glycosylated, 135-kDa ER-resident form of hERG (cg-hERG) was not altered upon short-term incubation, although it accumulated significantly on overnight exposure (16–24 h) to pentamidine (see Fig. 1, A and B), which is thought to be indicative of impaired forward trafficking.

To confirm independently that pentamidine inhibits hERG forward trafficking, we performed pulse-chase experiments to examine hERG maturation in the absence and presence of pentamidine. In these experiments, the appearance of complex or fully glycosylated hERG was used to monitor ER exit and passage of the channel protein through the Golgi apparatus. We found that hERG maturation from the initially synthesized 135-kDa ER resident form to the fully glycosylated 155-kD form was blocked, whereas the ER resident cg-form of hERG accumulated in the presence of 30 μM pentamidine (Fig. 2, A and B). To test whether inhibition of ER exit was also reflected in an altered subcellular localization of hERG, we costained HEK/hERG cells in immunocytochemical experiments with anti-hERG and anti-KDEL (a well established ER marker) antibodies either under control conditions or after overnight exposure to pentamidine (Fig. 2C). Although hERG staining could be detected both at the cell surface and in the ER under control conditions, hERG was restricted to the ER on incubation with pentamidine, as expected, when ER export is blocked.

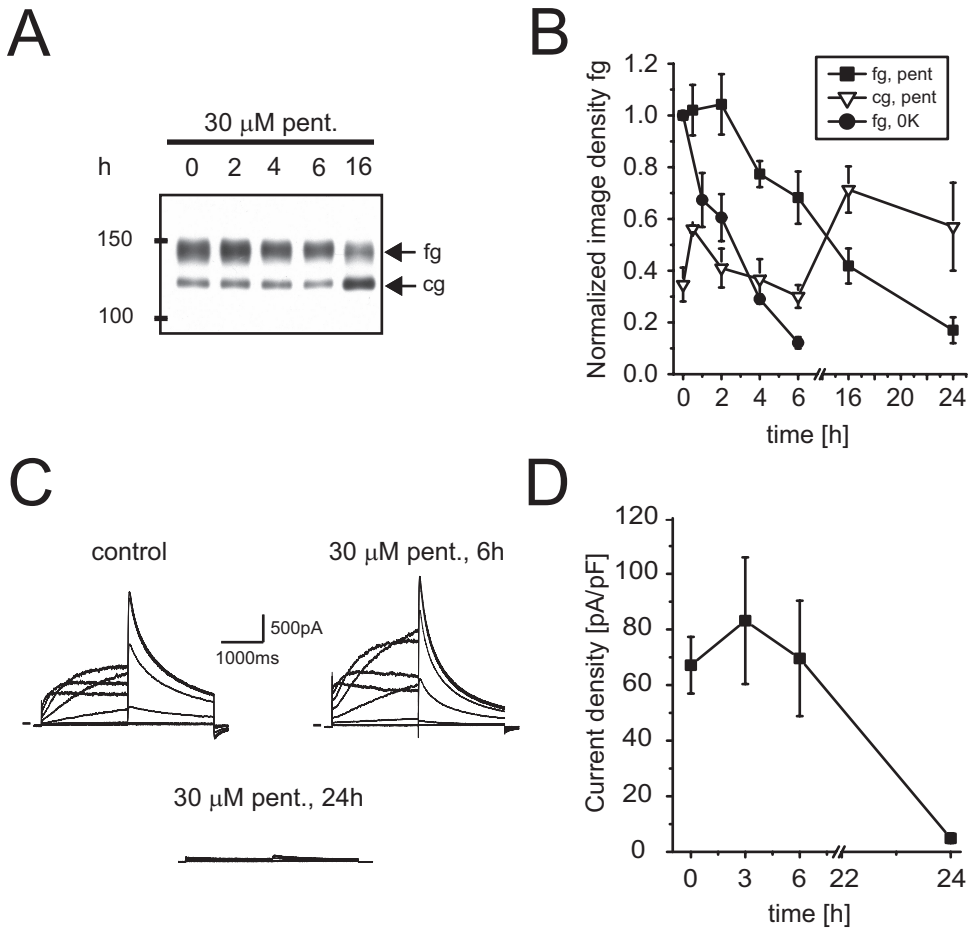

Fig. 1. Pentamidine does not reduce hERG surface expression on short-term exposure. A, Western blot showing time-dependent effects of incubation with 30 μM pentamidine (pent) on hERG stably expressed in HEK293 cells. B, quantitative analysis of time-dependent changes in fg- and cg-hERG levels after exposure to 30 μM pentamidine. Fast effects of 0 K^+ on fg-hERG (fg, 0K) are due to increased endocytic uptake. Image densities on Western blots were normalized to fg-hERG levels measured at $t = 0$. Note that cg-hERG is increased at $t = 16$ to 24 h ($n = 3$–4). C, representative hERG current families recorded under control conditions, after a 6- or 24-h (overnight) exposure to 30 μM pentamidine. Currents were elicited using depolarizing voltage steps from −60 to +60 mV. Tail currents were recorded on return to −50 mV. Holding potential was −80 mV. D, time-dependent reduction of hERG tail current densities on exposure to 30 μM pentamidine ($n = 6$–10). Data are given as mean ± S.E.

Astemizole Rescues Pentamidine-Induced Trafficking Inhibition. Astemizole is an antihistamine known to directly block hERG channels with high affinity in electrophysiological experiments, where IC_{50} values of 6 to 13 nM have been reported at physiological temperatures (hERGAP-Dbase; Hishigaki and Kuhara, 2011). More importantly, however, astemizole has been used previously as a pharmacological chaperone to correct trafficking defects in several LQTS-hERG mutations located in the transmembrane region of the channel protein, most likely via direct interactions with the universal drug binding site in the conduction pathway (Ficker et al., 2002). Consequently, we employed astemizole as a conformation-sensitive probe to further dissect inhibition of hERG forward trafficking by pentamidine. Astemizole restored hERG trafficking in the presence of 10 μM pentamidine half-maximally at a concentration of 335 ± 33 nM ($n = 3$) on Western blots. In the presence of 30 μM pentamidine, astemizole rescue was half-maximal at 962 ± 89 nM ($n = 3$) with the rescue-response curve parallel-shifted to the right (Fig. 3, A and B). Furthermore, astemizole was able to restore ER export to control levels at both pentamidine concentrations tested, as if pentamidine and astemizole were to compete for overlapping binding sites. To test whether pharmacological rescue would produce functional channels at the cell surface, we also measured hERG currents (Fig. 3C). Tail current density was 43.5 ± 4.4 pA/pF ($n = 7$) under control conditions and 4.9 ± 1.5 pA/pF ($n = 6$) after overnight incubation with 30 μM pentamidine. On coincubation with 30 μM pentamidine and 5 μM astemizole, tail current density was increased to 19.3 ± 4.3 pA/pF ($n = 6$) after astemizole had been washed out for 1 h before recording. Because washout of a high-affinity blocker such as astemizole is notoriously difficult and never complete, we also determined tail currents densities in HEK/hERG cells incubated solely with 5 μM astemizole. Under these conditions, we measured a current density of 16.4 ± 2.8 pA/pF ($n = 6$) after a 1-h washout of astemizole, which was not different from measurements that followed coincubation with both pentamidine and astemizole. Taken together, our data suggest that pentamidine-induced trafficking inhibition can be almost completely reversed by the pharmacological chaperone astemizole as judged from Western blots, and that fully functional channels are rescued to the cell surface.

Mutational Analysis of Pentamidine-hERG Interactions. Guided by our rescue experiments, we surveyed a series of mutations in the transmembrane domain of hERG (S1–S6) that replaced negatively charged glutamate or aspartate residues with alanine, because we considered negatively charged amino acid residues putative interaction partners for positively charged pentamidine. Mutations in the S1–S4 voltage sensor domain included hERG 4EC, which removes not one but four glutamate residues in the extracellular S1–S2 linker (Fernandez et al., 2005), hERG D456A, D460A, D466A, D509A, E518A, E519A, D540A, and E544A. In the inner pore region (S5–S6), we tested three additional negative charge replacements, hERG E575A, D580A, and D591A. We found that none of these mutations affected pentamidine-induced hERG trafficking inhibition (data not shown).

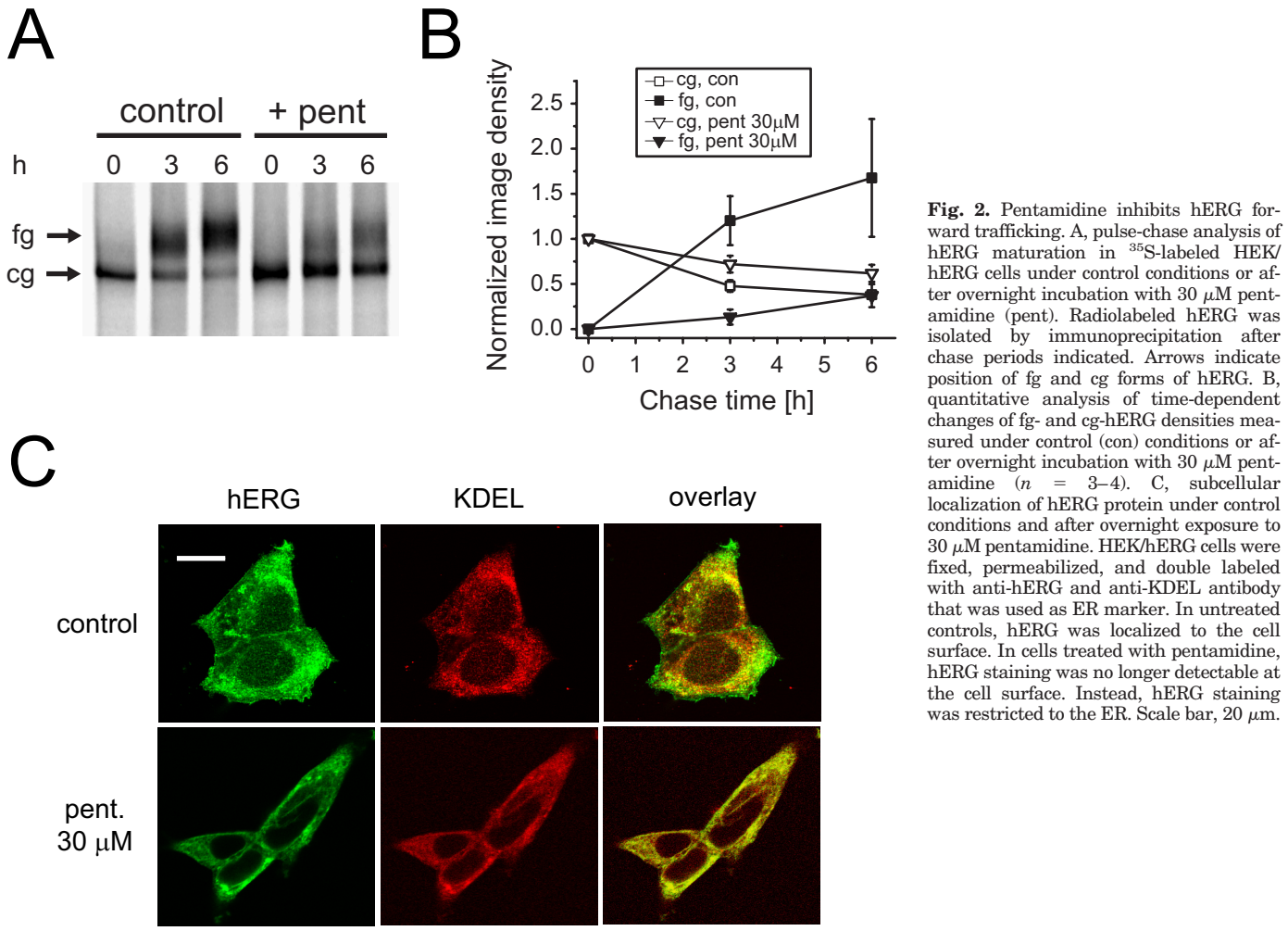

Fig. 2. Pentamidine inhibits hERG forward trafficking. A, pulse-chase analysis of hERG maturation in ^{35}S-labeled HEK/hERG cells under control conditions or after overnight incubation with 30 μM pentamidine (pent). Radiolabeled hERG was isolated by immunoprecipitation after chase periods indicated. Arrows indicate position of fg and cg forms of hERG. B, quantitative analysis of time-dependent changes of fg- and cg-hERG densities measured under control (con) conditions or after overnight incubation with 30 μM pentamidine (n = 3–4). C, subcellular localization of hERG protein under control conditions and after overnight exposure to 30 μM pentamidine. HEK/hERG cells were fixed, permeabilized, and double labeled with anti-hERG and anti-KDEL antibody that was used as ER marker. In untreated controls, hERG was localized to the cell surface. In cells treated with pentamidine, hERG staining was no longer detectable at the cell surface. Instead, hERG staining was restricted to the ER. Scale bar, 20 μm.

In marked contrast, pentamidine-induced trafficking inhibition was substantially attenuated by hERG F627Y, a unique mutation in the signature sequence of the selectivity filter (Fig. 4; Supplemental Fig. S1). HERG F627Y was selected for analysis because it rendered channels less sensitive toward cardiac glycosides, another well characterized class of hERG trafficking inhibitors (Wang et al., 2007, 2009). Because F627Y promotes channel inactivation (Gang and Zhang, 2006), we extended our analysis to hERG S641A, a mutation in the S6 transmembrane helix with accelerated inactivation (Fig. 4B; Supplemental Fig. S2) (Bian et al., 2004), and to hERG S631A, a mutation in the extracellular mouth of the conduction pathway with disrupted inactivation (Zou et al., 1998). In both instances, we found wild-type behavior suggesting that pentamidine effects were not correlated with inactivation gating (Fig. 4, B and C; Supplemental Fig. S1).

Next, we focused on the possibility that astemizole and pentamidine may share overlapping binding sites. We approached this hypothesis in a first set of experiments using bEAG channels instead of engineered hERG mutants. This is for the following reason: both hERG and bEAG belong to the EAG potassium channel family and show a high degree of sequence homology in the inner pore region (S5–S6), where the canonical drug binding site of hERG is located (Warmke and Ganetzky, 1994). However, bEAG channels are relatively insensitive to block by "classic" hERG blockers (Ficker et al., 1998). Likewise, astemizole blocks hERG half-maximally at concentrations of 6 to 13 nM, whereas hEAG is approximately 20 to 30 times less sensitive, with an IC_{50} value of approximately 200 nM (García-Ferreiro et al., 2004). Thus, we speculated that bEAG may be less sensitive to pentamidine-induced trafficking inhibition, if a hERG-like drug binding site were to form an indispensable mechanistic requirement. Indeed, bEAG trafficking was not affected by pentamidine concentrations up to 100 μM as judged from analysis of fully glycosylated cell surface channels on Western blots (Fig. 4, A and B). Furthermore, bEAG currents were much less sensitive on long-term exposure to pentamidine than hERG WT channels (Fig. 4C).

At this point, our structure-function studies directed us toward the universal drug binding site of hERG as a candidate region for pentamidine interactions. The two most important determinants of drug binding to hERG include an aromatic tyrosine (Tyr652) and phenylalanine (Phe656) in the S6 transmembrane helix that are complemented by additional residues located at the intracellular mouth of the selectivity filter (Thr623, Ser624, Val625) when high-affinity blockers such as astemizole are bound (Mitcheson et al., 2000). We studied the effects of mutations in three positions, hERG Ser624, Tyr652, and Phe656, to evaluate the effects of perturbations of drug binding on pentamidine-induced trafficking inhibition. When hERG S624A was transiently ex-

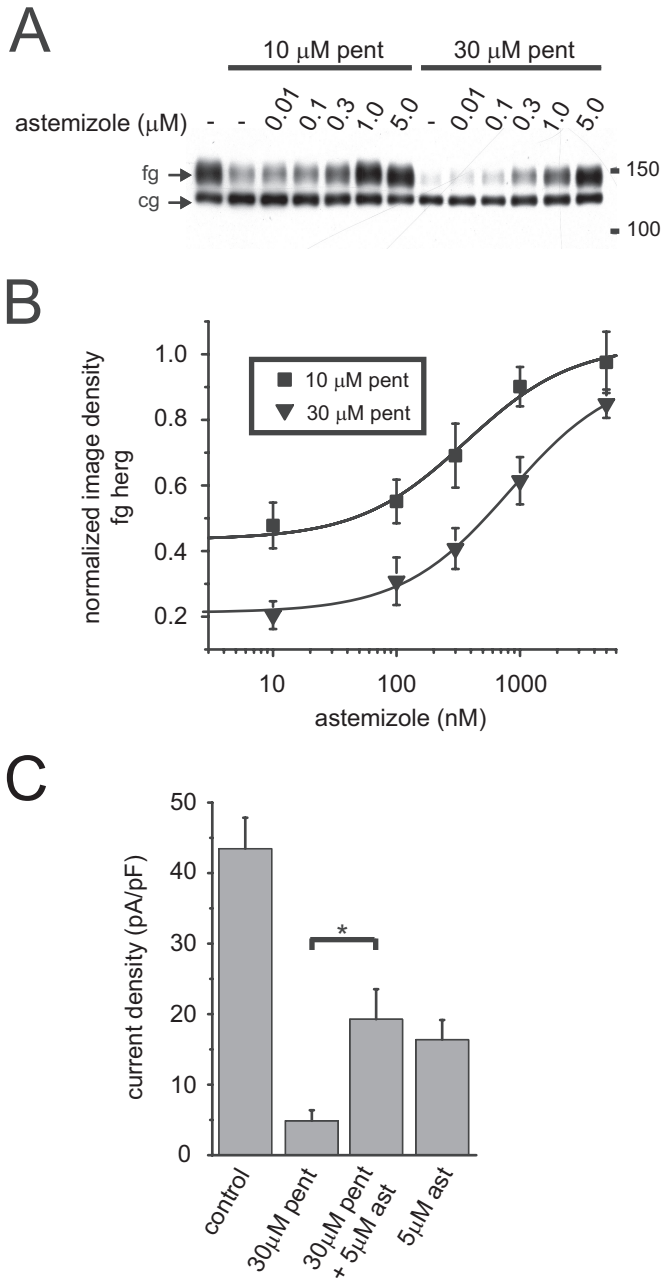

Fig. 3. Rescue of pentamidine-induced trafficking inhibition by incubation with the pharmacological chaperone astemizole. A, Western blot showing effects of overnight treatment with increasing concentrations of astemizole (ast) on HEK/hERG cells coincubated with either 10 or 30 μM pentamidine (pent). B, quantitative analysis of concentration-dependent rescue of fg-hERG by astemizole after coincubation with either 10 or 30 μM pentamidine. Astemizole restored hERG trafficking in the presence of 10 μM pentamidine half-maximally at a concentration of 335 $\pm$ 33 nM (n = 3). In the presence of 30 μM pentamidine, astemizole rescue was half-maximal at 962 $\pm$ 89 nM (n = 3). C, maximal hERG tail current densities measured on return to $-$50 mV (holding potential was $-$80 mV; 2-s depolarizing test pulses) under control conditions, on overnight incubation with 30 μM pentamidine, 30 μM pentamidine + 5 μM astemizole (washout, 1 h) and 5 μM astemizole to determine residual block after 1 h washout (n = 6–7). Note that coincubation with 5 μM astemizole significantly increased hERG tail currents after overnight incubation with 30 μM pentamidine. Current densities measured on rescue were not significantly different from densities measured on incubation with astemizole alone.

pressed in HEK cells and exposed overnight to either 10 or 30 μM pentamidine, fg-hERG S624A levels were reduced on Western blots to 61 $\pm$ 4.5 and 36 $\pm$ 5.2% (n = 3), respectively, which was not different from WT levels, which were reduced to 61 $\pm$ 3.8 and 33 $\pm$ 3.9% (n = 5–6; Supplemental Fig. S3).

Our Western analysis of hERG Y652A revealed an unusual biphasic change in surface expression on overnight incubation with pentamidine; i.e., an initial increase in cell surface hERG Y652A on incubation with 1 μM pentamidine was followed by a decrease with 10 and 30 μM pentamidine. In marked contrast, expression of the immature (cg) form of hERG Y652A was augmented in a dose-dependent manner over the entire concentration range studied (Supplemental Fig. S4). The biphasic behavior of fg-hERG Y652A on Western blots was also reflected in electrophysiological recordings, where tail current density increased from $-$31 $\pm$ 5.0 pA/pF (n = 14) under control conditions to $-$102.7 $\pm$ 19.5 pA/pF (n = 4) on overnight incubation with 1 μM pentamidine, followed by a decrease to $-$75.3 $\pm$ 13.8 (n = 11) and $-$48 $\pm$ 6.6 pA/pF (n = 14) on incubation with 10 and 30 μM pentamidine, respectively.

Next, we analyzed a series of point mutations in position Phe656, which is crucial to drug binding in hERG, including substitutions with tryptophan, methionine, threonine, cysteine, alanine, and valine (Fernandez et al., 2004; Guo et al., 2006). In general, high-affinity drug binding is believed to be correlated with measures of hydrophobicity. Specifically, it has been reported that IC_{50} values for several high-affinity blockers were increased when Phe656 was mutated to Thr, Ala, or Val. We transiently expressed all six point mutations in HEK293 cells, exposed them overnight to either 10 or 30 μM pentamidine, and analyzed the amount of mature fg-hERG on Western blots (Fig. 5A). We found that substitutions in 656 with Thr, Cys, Ala, or Val produced channels apparently less sensitive to pentamidine than WT or channels with substitutions of Trp or Met (Fig. 5B). To correlate changes in surface expression with changes in current expression, we also recorded maximal tail current amplitudes at $-$120 mV under control conditions or on incubation with either 10 or 30 μM pentamidine (Fig. 5C; Supplemental Fig. S5). In line with our Western analysis, we found that three substitutions, threonine, cysteine, and valine, were significantly less sensitive to pentamidine than WT or 656Trp and 656Met mutant channels.

How Does Pentamidine Interfere with ER Export of hERG? To gain first insight of how pentamidine binding may be translated into inhibition of ER export, we tested, whether pentamidine destabilizes tetrameric channel assembly, thereby producing incompletely assembled proteins that are retained in the ER. To assess the oligomerization state of hERG, we separated digitonin lysates of HEK/hERG cells incubated in the absence and presence of 30 μM pentamidine on sucrose gradients. Figure 6 shows a Western analysis of brefeldin A-treated hERG gradient fractions, illustrating the distribution of hERG in two prominent protein peaks, P1 and P2, with the majority of hERG protein present in P2. Using Blue Native-PAGE, we have previously determined that hERG is present as monomer or dimer in peak P1, whereas it forms channel tetramers in P2 (Wang et al., 2009). It is noteworthy that we could detect no quantitative differences in the distribution of hERG on sucrose gradients as a consequence of pentamidine exposure. To evaluate the sensitivity of our assay, we also studied a trafficking impaired LQTS2 mutation, hERG A561V (Ficker et al., 2000). Compared with WT, HERG A561V showed an increase in peak P1 with a

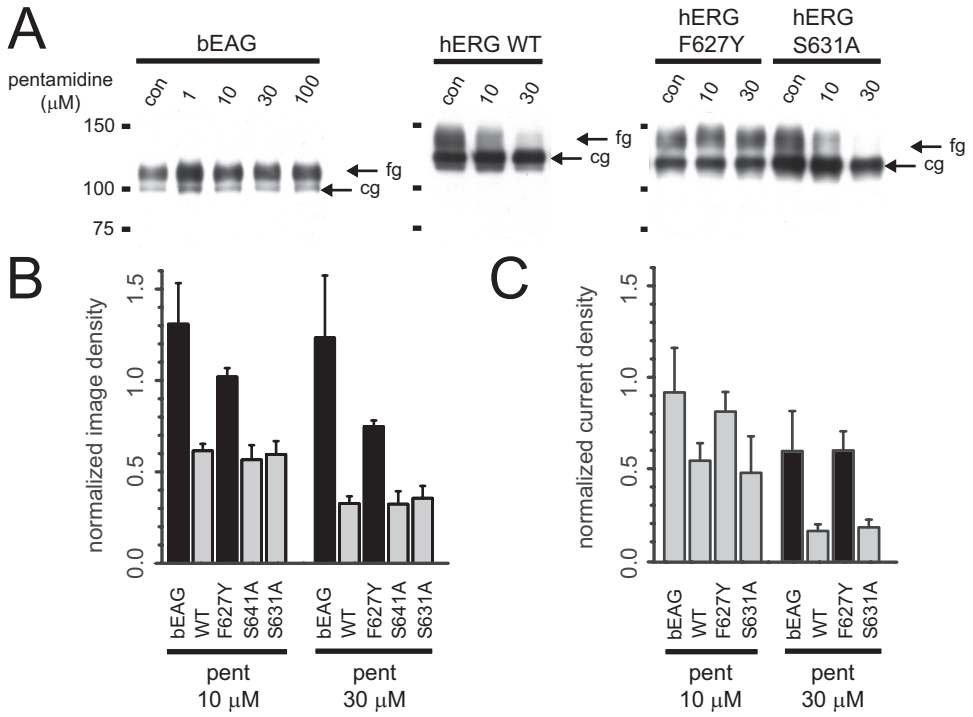

Fig. 4. A mutation in the selectivity filter alters sensitivity of hERG to pentamidine induced trafficking inhibition. A, Western blots showing effects of overnight treatment with increasing concentrations of pentamidine on bEAG, hERG WT, hERG F627Y, and hERG S631A transiently expressed in HEK293 cells. B, quantitative analysis of fully glycosylated form of bEAG ($n = 3$), hERG WT ($n = 5–6$), hERG F627Y ($n = 6$), hERGS641A ($n = 4$), and hERG S631A ($n = 3$) after long term-exposure to 10 and 30 μM pentamidine (pent). Image densities of fully glycosylated protein bands on Western blots were captured using a Kodak Imager, quantified, and normalized to untreated controls. Black bars indicate a significant difference between fg-WT and bEAG or fg-hERG F627Y on treatment with either 10 or 30 μM pentamidine (Dunnett's t test; $p < 0.05$). C, hERG WT ($n = 7–8$), bEAG ($n = 6–7$) and hERG S631A (7–9) currents were activated in the presence of 5 mM $[K^+]_{ex}$ from a holding potential of −80 mV with depolarizing pulses (2 s). Maximal hERG WT tail current amplitudes were recorded on return to −120 mV. BEAG and hERG S631A current amplitudes were recorded at the end of depolarizing pulses to +20 mV. For hERG F627Y ($n = 9–7$) maximal tail current amplitudes were recorded on return to −80 mV in the presence of 140 mM $[K^+]_{ex}$. Tail current amplitudes were converted into current densities and normalized to amplitudes measured in untreated controls. Black bars indicate a significant difference between WT and bEAG or hERG F627Y current densities on exposure to 30 μM pentamidine (Dunnett's t test; $p < 0.05$).

concomitant reduction in P2 indicating that assembly of this trafficking-deficient LQTS2 mutant was destabilized (Supplemental Fig. S6).

Other possible explanations for ER retention include 1) inhibition of chaperone association in the hERG export pathway as described for geldanamycin or 2) drug-induced channel misfolding leading to prolonged hERG-chaperone interactions and ER retention (Ficker et al., 2003). Consequently, we studied interactions of hERG WT with two major cytosolic chaperones, Hsp/c70 and Hsp90, immediately after synthesis, or after a chase period of 6 h in HEK/hERG cells cultured under control conditions or after overnight incubation with pentamidine (Fig. 7A). Quite surprisingly, we found no difference in the formation and stability of either hERG/Hsp/c70 or hERG/Hsp90 complexes in the presence of pentamidine (Figs. 7B). Thus, pentamidine-induced inhibition of hERG forward trafficking may not be mediated via cytosolic chaperones.

Finally, inhibition of ER export has often been linked to increased channel ubiquitination (Ficker et al., 2003; Gong et al., 2005). Consequently, we measured hERG ubiquitination under control conditions or after overnight exposure to 30 μM pentamidine. To this end, we expressed hERG WT together with HA- or His_6- tagged ubiquitin. Incubation with the Hsp90 inhibitor geldanamycin, known to increase hERG ubiquitination, was used as positive control. After immunoprecipitation with anti-hERG antibody immunoprecipitates were blotted with either anti-hERG or anti-HA antibody to detect multiubiquitinated hERG proteins. We found that on Western blots, hERG ubiquitination was increased in the presence of geldanamycin but not pentamidine (Fig. 8), which actually decreased hERG ubiquitination slightly.

Analysis of Pentamidine Effects on Native hERG/I_{Kr} Currents in Cardiomyocytes. In addition to our experiments in a heterologous expression system, we have also studied pentamidine effects on native ERG protein and I_{Kr} currents in murine HL-1 cardiac myocytes (Claycomb et al., 1998) as well as in NRVMs. To assess for pentamidine-induced inhibition of channel surface expression, we incubated HL-1 cells overnight with either 1 or 10 μM pentamidine. On Western blots, we found that pentamidine suppressed expression of fully glycosylated full-length mERG1a protein as well as of an N-terminal splice variant, mERG1b, present in HL-1 myocytes in a concentration-dependent manner. In contrast, Kv1.5 expression was not altered by incubation with pentamidine (Fig. 9A). Reduction of cell surface mERG was associated with suppression of the corresponding native ion current, I_{Kr}, as expected. After depolarizing steps from a holding potential of −80 mV slow tail currents were activated on return to −50 mV that specifically reflect ERG-mediated I_{Kr} (Fig. 9B, arrows). Maximal I_{Kr} density was reduced from 3.9 ± 0.6 pA/pF ($n = 14$) under control conditions to 0.6 ± 0.1

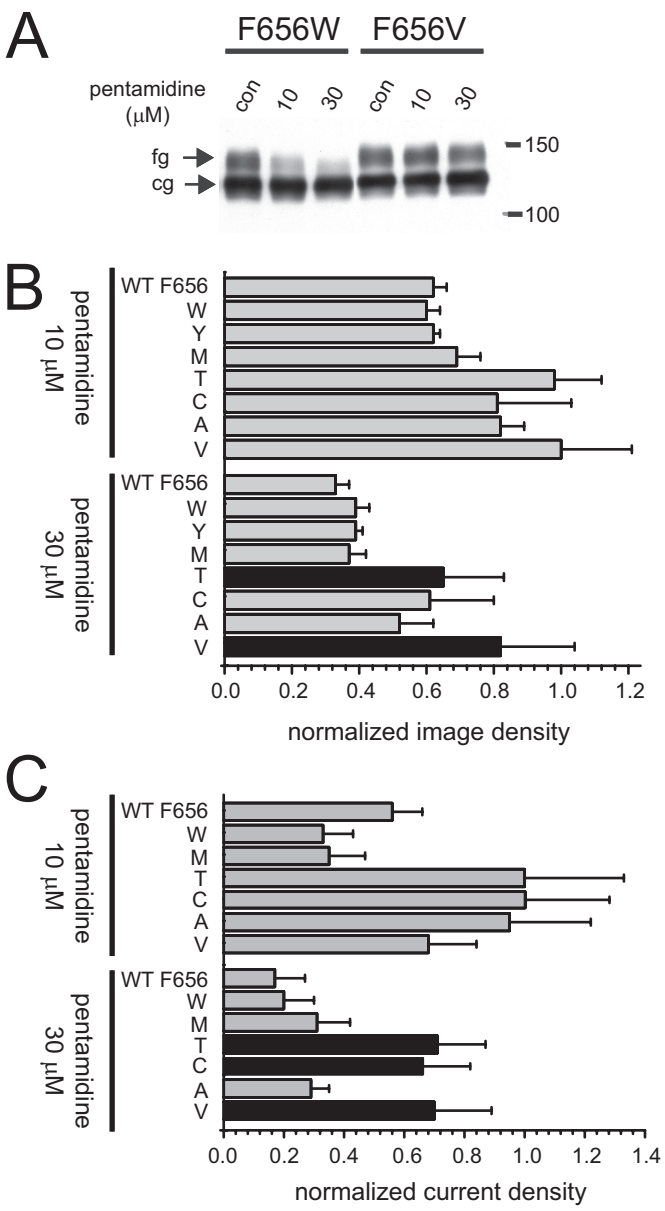

Fig. 5. Mutation of Phe656 in S6 transmembrane helix alters sensitivity to pentamidine-induced trafficking inhibition. A, Western blot showing effects of overnight treatment with increasing concentrations of pentamidine on hERG F656W and hERG F656V transiently expressed in HEK293 cells. B, quantitative analysis of fg form of hERG Phe656 (WT, $n = 5–6$), hERG 656Trp ($n = 5$), 656Tyr ($n = 4$), 656Met ($n = 3$), 656Thr ($n = 4$), 656Cys ($n = 3$), 656Ala ($n = 3$), and 656Val ($n = 4$) after overnight treatment with 10 or 30 μM pentamidine. Image densities of fully glycosylated protein bands on Western blots were captured using a Kodak Imager, then quantified and normalized to untreated controls. Black bars indicate a significant difference between fg-Phe656 (WT) and fg-656Thr and 656Val on treatment with 30 μM pentamidine (Dunnett's t test; $p < 0.05$). C, WT ($n = 7–8$) or mutant currents (Trp, $n = 6–8$; Met, $n = 7–8$; Thr, $n = 7–12$; Cys, $n = 4–6$; Ala, $n = 6–8$; Val, $n = 5–7$) were activated in the presence of 5 mM $[K^+]_{ex}$ from a holding potential of −80 mV with a depolarizing pulse to + 60 mV (2 s). Tail currents were recorded on return to −120 mV. Tail current amplitudes were converted into current densities and normalized to amplitudes measured under control conditions. Black bars indicate a significant difference between WT and F656T, F656C, and F656V on treatment with 30 μM pentamidine (Dunnett's t test; $p < 0.05$).

pA/pF ($n = 5$) after overnight incubation with 10 μM pentamidine (Fig. 9C). When I_{Kr} was blocked by application of 5 μM E4031, residual I_K currents were analyzed at the end of depolarizing test pulses to +60mV. In contrast to I_{Kr}, I_K current density was not significantly affected by 10 μM pentamidine. We measured 8.8. ± 2.7 pA/pF ($n = 7$) under control conditions and 11.8 ± 3.6 pA/pF ($n = 6$) on incubation with 10 μM pentamidine.

Furthermore, we have studied pentamidine effects on native I_{Kr}/rERG channels in cultured NRVMs. Overnight incubation with pentamidine (30 μM) suppressed the fully glycosylated (fg) cell surface form of rERG on Western blots. It is noteworthy that pentamidine effects could be reversed on coincubation with 3 μM astemizole, as expected from our experiments with HEK/hERG cells (Fig. 9D). To complement our Western analysis in NRVMs, we also monitored I_{Kr} current density as a function of pentamidine exposure. NRVM I_{Kr} currents were isolated in symmetrical Cs^+-solutions and elicited using 350-ms depolarizing test pulses from a holding potential of −80 mV (Fig. 9E). Maximal I_{Kr} tail current amplitudes measured on return to −80 mV were reduced from −16.5 ± 3.1 pA/pF ($n = 5$) under control conditions to −6.8 ± 1.6 pA/pF ($n = 5$) after overnight incubation with 30 μM pentamidine (Fig. 9F).

Discussion

Pentamidine is unusual in that it targets the cardiac potassium channel hERG by reducing its surface expression slowly over time, which delays cardiac repolarization and contributes to prolongation of the QT interval on the electrocardiogram (Cordes et al., 2005; Kuryshev et al., 2005). To contrast this unique mode of action with direct hERG blockade, pentamidine has been classified in the past as a hERG trafficking inhibitor, which tacitly implied disruption of forward trafficking from the ER as mechanism. However, channel endocytosis in combination with accelerated degradation has emerged more recently as an alternative mechanism used by proarrhythmic compounds to control hERG surface expression. For example, it has been shown that probucol, a cholesterol-lowering drug causing acLQTS, increased endocytic hERG uptake from the cell surface (Guo et al., 2011). A similar increase in endocytosis has been described upon exposure of hERG to low extracellular potassium concentrations (Guo et al., 2009). To clarify the cellular and molecular mechanisms that control hERG surface expression in the presence of pentamidine, we have investigated the time course of pentamidine effects on Western blots and in electrophysiological current recordings. In contrast to fast changes in surface expression seen with probucol or on incubation with 0 $[K^+]_{ex}$, short-term effects of pentamidine were minimal over several hours and consistent with a half-life of approximately 10 to 11 h determined for WT under control conditions (Ficker et al., 2003). It is noteworthy that lack of short-term effects cannot be attributed to slow access of dicationic pentamidine to the cell interior, because acute inward rectifier block was established within 5 to 10 min after extracellular application of pentamidine (Cordes et al., 2005; Kuryshev et al., 2005; de Boer et al., 2010). Furthermore, we have shown that newly synthesized hERG did not reach the Golgi apparatus using pulse chase experiments and that hERG immunostaining was restricted to the ER in the presence of pentamidine. Thus, we conclude that pentamidine disrupts exclusively hERG forward trafficking from the ER.

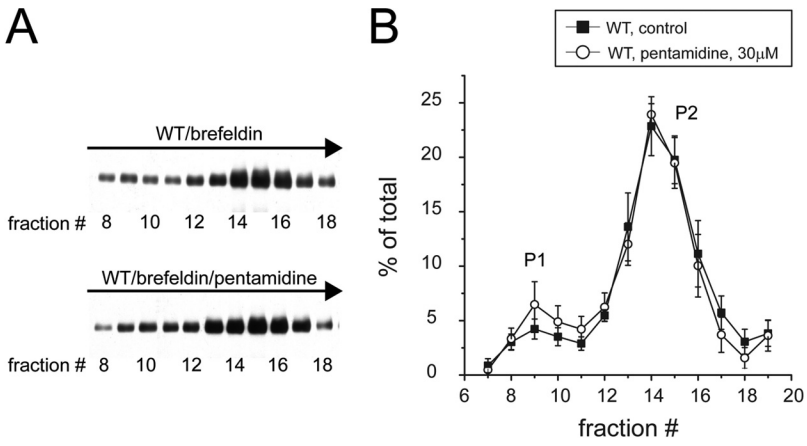

Fig. 6. Long-term exposure to pentamidine does not alter tetrameric structure of hERG. A, sedimentation analysis of heterologously expressed hERG WT channels incubated overnight either in the presence of 1 μg/ml brefeldin A to inhibit complex glycosylation of the channel protein or in a combination of 1 μg/ml brefeldin A and 30 μM pentamidine. Digitonin lysates were separated on 15 to 45% sucrose gradients. Gradient fractions were analyzed by Western blotting using anti-hERG antibody. Arrow indicates the direction of sedimentation. Fraction numbers are indicated below the Western blot. Image densities of gradient fractions were analyzed using a Kodak Imager. B, quantification of steady-state sedimentation gradients as shown in A. Signals from an entire gradient were summed up and set at 100% (total). Individual signals in each fraction were expressed as a percentage of total. P1 and P2 denote two major hERG peaks corresponding to channel monomers/dimers (P1) and channel tetramers (P2) (n = 3).

To further dissect inhibition of forward trafficking by pentamidine at the mechanistic level, we have used the pharmacological chaperone astemizole as a conformation-sensitive probe. Astemizole has been used previously to correct conformational defects in misfolded, trafficking-deficient LQTS hERG mutants, whereas folding and trafficking of wild-type channels were not affected (Ficker et al., 2002). In addition, astemizole rescue was restricted to mutations in the transmembrane domain of the channel protein (Anderson et al., 2006) and relied on binding to Phe656 in the universal drug binding site of hERG (Ficker et al., 2002). By analogy, we speculated that successful rescue experiments with astemizole might help us to uncover and localize pentamidine-induced conformational defects in hERG. In fact, astemizole restored hERG trafficking in the presence of pentamidine indicating first of all that a "general" shut down of protein export from the ER was not the root cause for pentamidine-induced trafficking inhibition. This was not unexpected, because pentamidine reduced hERG surface expression specifically among several other major cardiac ion channels tested (Kuryshev et al., 2005). More importantly, however, successful astemizole rescue suggested an induced conformational defect in the transmembrane region of hERG and provided first hints that astemizole and pentamidine may interact in a competitive manner.

Several predictions from rescue experiments could be verified directly in our mutational analysis. First, pentamidine

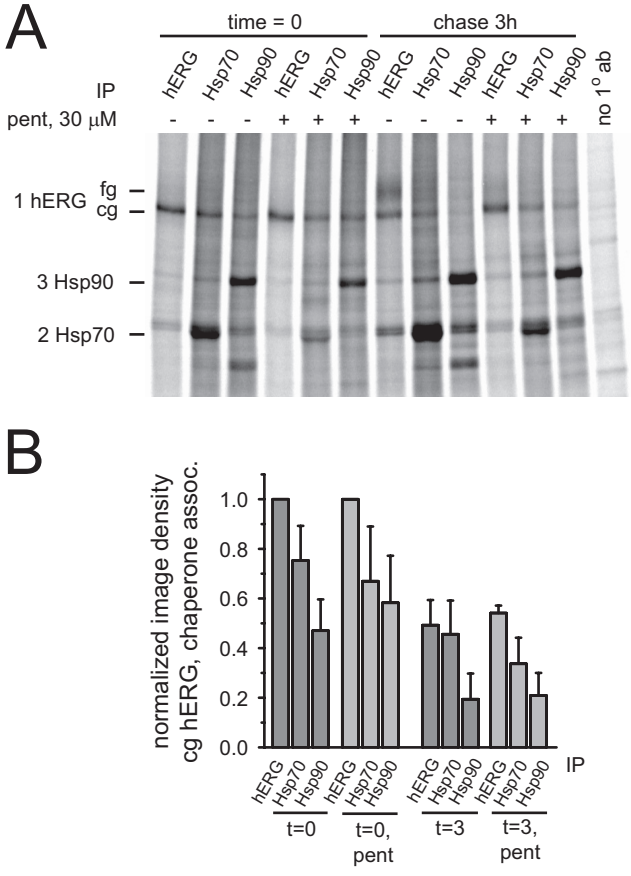

Fig. 7. Pentamidine does not interfere with Hsp/c70 and Hsp90 function. A, shown is a pulse-chase experiment performed in the absence and presence of 30 μM pentamidine (pent). Radiolabeled hERG protein was isolated using immunoprecipitation with anti-hERG, anti-Hsp/c70, or anti-Hsp90 antibody after chase periods indicated. Left, positions of fg/cg hERG, Hsp/c70, and Hsp90 on the autoradiogram are indicated. Rightmost lane represents a negative control with no primary antibody added. B, quantitative analysis of time-dependent formation of hERG-Hsp/c70 and hERG-Hsp90 complexes in the absence and presence of pentamidine (n = 3–4). Note that chaperone association is not different between control and pentamidine treated cells.

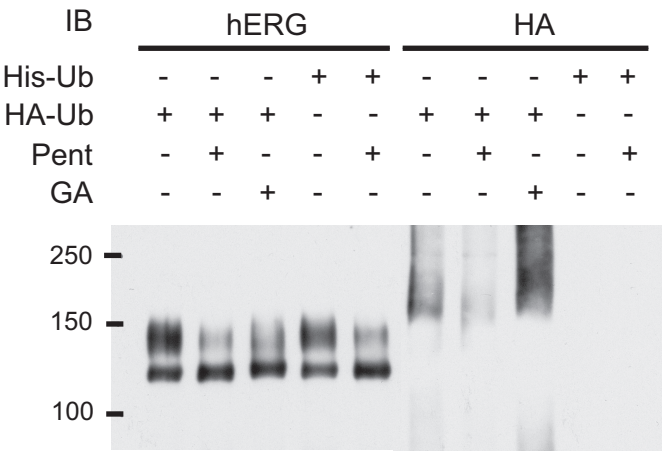

Fig. 8. Pentamidine does not increase HERG ubiquitination. Western blot analysis of HEK/hERG cells transiently transfected with HA-tagged ubiquitin (HA-Ub) and treated overnight with either 30 μM pentamidine (Pent) or 10 μM geldanamycin (GA) used as positive control. Transfection with His_6-ubiquitin was used as negative control. Whole-cell lysates were immunoprecipitated with anti-hERG antibody, resolved by SDS-PAGE, and immunoblotted (IB) using either anti-hERG antibody (hERG-IP) or HA-Ub. Immunoblotting with anti-HA antibody identifies high-molecular-weight forms of ubiquitinated hERG that are increased on treatment with geldanamycin but not pentamidine.

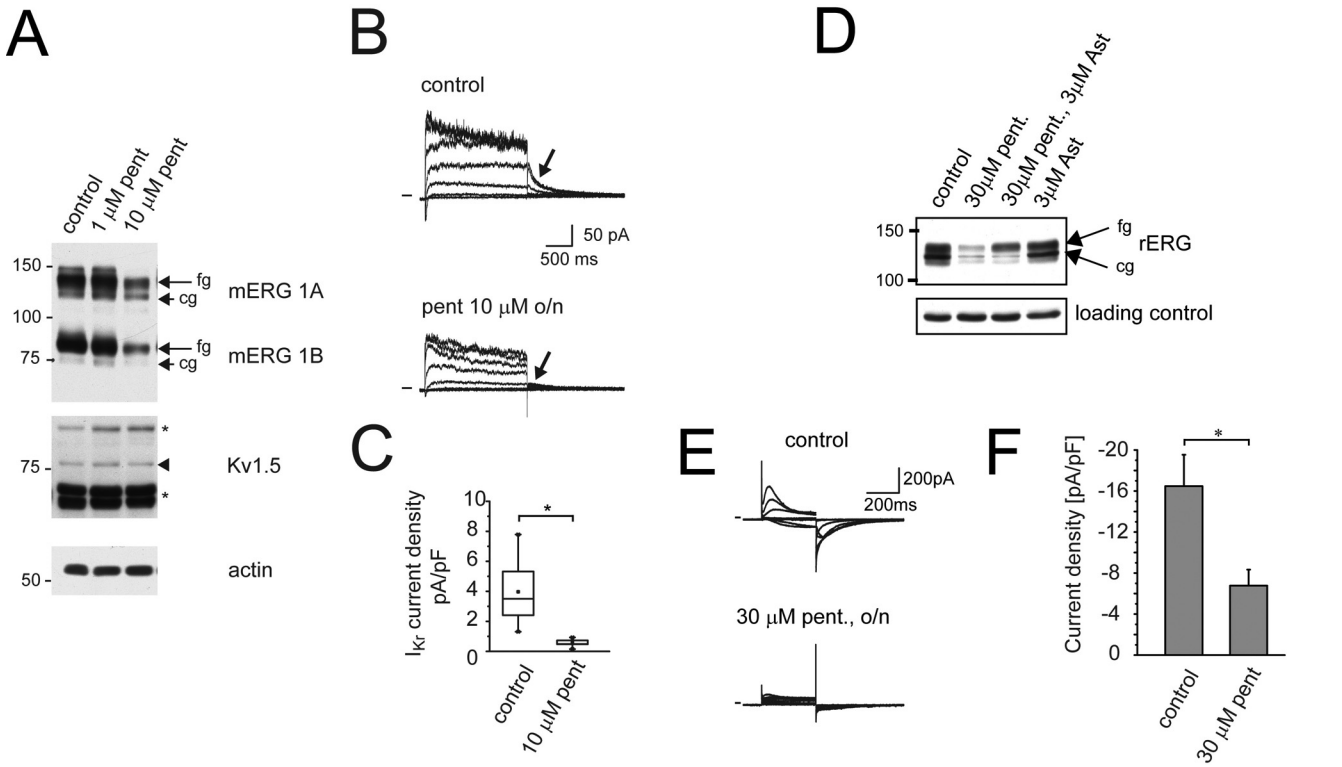

Fig. 9. Pentamidine suppresses endogenous ERG/I_{Kr} currents in HL-1 cardiomyocytes and in NRVMs. A, Western blot showing mERG in HL-1 cardiomyocytes under control conditions and after overnight exposure to either 1 or 10 μM pentamidine (pent). Note that both mERG1A and mERG1B were reduced by pentamidine, whereas mKv1.5 was not affected. Actin was used as loading control. B, mERG currents recorded in HL-1 cardiomyocytes under control conditions or after overnight exposure to 10 μM pentamidine. Currents were elicited using 2-s depolarizing test pulses from -60 to $+60$ mV. Holding potential was -80 mV. Tail currents were recorded on return to -50 mV. C, quantitative analysis of maximal mERG tail current densities under control conditions or after overnight exposure to 10 μM pentamidine ($n = 6–7$). Data are represented in statistical box blots. Note that current densities were significantly different at $p < 0.05$ level. D, Western blot showing rERG in NRVMs under control conditions and after overnight exposure to 30 μM pentamidine, to 30 μM pentamidine + 3 μM astemizole (Ast), and to 3 μM astemizole alone. Note that coincubation with astemizole rescued fg-rERG in the presence of pentamidine. E, rERG currents in NRVMs were elicited in symmetric Cs^+ solutions using depolarizing test pulses from -60 to $+60$ mV. Holding potential was -80 mV. F, quantitative analysis of maximal rERG tail current densities recorded on return to -80mV under control conditions or after overnight exposure to 30 μM pentamidine ($n = 5$). Data are given as mean ± S.E. Note that current densities were significantly different at $p < 0.05$ level.

effects were attenuated by hERG F627Y, a mutation in the narrow selectivity filter. Because the amino acid residue in hERG627 does not project in the direction of the conduction pathway, it is accessible to neither dicationic pentamidine nor astemizole. However, a tyrosine residue in hERG627 may provide additional hydrogen bonds to a cuff of aromatic residues that stabilizes the selectivity filter and ultimately the entire channel protein (Doyle et al., 1998). This may also explain why hERG F627Y attenuates not only pentamidine effects but also trafficking defects induced by cardiac glycosides or on exposure to low K^+ (Wang et al., 2009; Massaeli et al., 2010).

Second, pentamidine effects were reduced by mutations in position hERG Phe656 that retained relatively normal biophysical properties but decreased sensitivity to direct hERG block (Fernandez et al., 2004). This suggested to us that a binding event similar to the binding of direct blockers in native channels may render hERG trafficking deficient. For example, mutation of Phe656 to Tyr, Trp, or Met did not affect pentamidine-induced trafficking inhibition, in line with only modest effects on direct hERG block. In contrast, mutation of Phe656 to Thr, Cys, or Val, all of which are relatively insensitive to drug block, strongly reduced trafficking inhibition. We also noted differences in the requirements for trafficking inhibition and drug binding. For example, mutation of Phe656 to Ala seemed to attenuate trafficking inhibition on Western blots but not in current recordings, although it has been shown to decrease direct hERG block very strongly. Likewise, the aromatic side chain in position 652 that is required to maintain drug sensitivity for high-affinity blockers such as (+)-*N*-[1′-(6-cyano-1,2,3,4-tetrahydro-2(*R*)-naphthalenyl)-3,4-dihydro-4(*R*)-hydroxyspiro(2*H*-1-benzopyran-2, 4′-piperidin)-6-yl]methanesulfonamide] monohydrochloride (MK-499) or cisapride (Mitcheson et al., 2000) was less important for pentamidine induced trafficking inhibition, because hERG Y652A retained at least some sensitivity to pentamidine.

Differences between the mechanisms of direct channel blockade and pentamidine-induced trafficking inhibition were anticipated, because terminally folded hERG channels are not blocked by pentamidine with high affinity in acute experiments (Cordes et al., 2005). In fact, the affinity of pentamidine for direct hERG block at physiological temperature was approximately 300 μM, whereas hERG trafficking was inhibited half-maximally only by 8 μM pentamidine (Kuryshev et al., 2005). For this reason, we propose that pentamidine binds to an emerging "universal drug binding site" in a folding intermediate of hERG with higher affinity than to the native conformation present in the terminally folded channel protein. We speculate that pentamidine binding arrests conformational maturation of hERG at a level

where channels are not yet exportable from the ER. The pharmacological chaperone astemizole on the other hand rescues pentamidine-induced trafficking inhibition by competing with pentamidine for an at least partially overlapping binding site. However, while astemizole facilitates channel maturation, pentamidine binding abrogates it, which is conceptually similar to the binding of an inverse agonist to its receptor target.

This leaves us with the important question of how ER export of hERG is curtailed by cellular quality control mechanisms in the presence of pentamidine. Obviously, the proposed interactions of pentamidine with residues in transmembrane helix S6 could have destabilized channel assembly, producing incompletely assembled proteins that are retained in the ER. However, we showed that hERG assembly into tetramers was not disturbed on long-term exposure to pentamidine. Alternatively, pentamidine could have arrested hERG in a slightly aberrant tetrameric conformation that is recognized by cellular chaperones. To our surprise, however, association with two crucial cytosolic chaperones, Hsp/c70 and Hsp90, was not altered in the presence of pentamidine. Although it is still possible that interactions with another chaperone system are targeted by pentamidine, we consider this possibility unlikely, because altered chaperone interactions are most often accompanied by an increase in channel ubiquitination and degradation. Again, this could not be shown. In marked contrast, channel ubiquitination was decreased, and immature, ER-resident hERG accumulated in the presence of pentamidine (Fig. 2B). On the basis of these observations, we suggest that long-term exposure to pentamidine may uncover a chaperone-independent quality control step for hERG. We believe that in the presence of pentamidine hERG matures to a point where chaperone systems disengage and where channels are subjected to a last quality check that does not focus on conformational integrity. Instead, channel proteins may be surveyed for exposed ER retention or export signals similar to what has been described for various inward rectifier channels.

Taken together, we have shown that in the presence of pentamidine hERG is no longer exported from the ER. Thus, inhibitors of hERG surface expression can be grouped in at least two functional classes: those that reduce hERG surface expression by increasing channel endocytosis, and those such as pentamidine or arsenic trioxide that prevent channel export from the ER and are best characterized as hERG trafficking inhibitors. Furthermore, we provide the first example of a therapeutic compound that arrests hERG maturation in a nonexportable form via binding to residues in the canonical drug-binding site of hERG. This is very different from what has been proposed for proarrhythmic compounds such as probucol or progesterone (Guo et al., 2011; Wu et al., 2011), which are thought to mediate changes in hERG surface expression via effects on the composition of lipid rafts surrounding the channel protein. The reliance of pentamidine on hERG-specific amino acid residues may also provide an answer to its specificity and may explain why pentamidine effects are restricted to ER export, because the native conformation of hERG that is present in post-ER compartments binds pentamidine with much lower affinity only.

Acknowledgments

HA- and His_6- ubiquitin cDNAs were kindly provided by D. Bohmann.

Authorship Contributions

Participated in research design: Deschenes and Ficker.
Conducted experiments: Dennis, Wang, Wan, Nassal, and Ficker.
Performed data analysis: Dennis, Wang, Wan, and Ficker.
Wrote or contributed to the writing of the manuscript: Deschenes and Ficker.

References

Anderson CL, Delisle BP, Anson BD, Kilby JA, Will ML, Tester DJ, Gong Q, Zhou Z, Ackerman MJ, and January CT (2006) Most LQT2 mutations reduce Kv11.1 (hERG) current by a class 2 (trafficking-deficient) mechanism. *Circulation* **113:** 365–373.
Barbey JT, Pezzullo JC, and Soignet SL (2003) Effect of arsenic trioxide on QT interval in patients with advanced malignancies. *J Clin Oncol* **21:**3609–3615.
Bian JS, Cui J, Melman Y, and McDonald TV (2004) S641 contributes HERG K+ channel inactivation. *Cell Biochem Biophys* **41:**25–40.
Bibler MR, Chou TC, Toltzis RJ, and Wade PA (1988) Recurrent ventricular tachycardia due to pentamidine-induced cardiotoxicity. *Chest* **94:**1303–1306.
Burchmore RJ, Ogbunude PO, Enanga B, and Barrett MP (2002) Chemotherapy of human African trypanosomiasis. *Curr Pharm Des* **8:**256–267.
Claycomb WC, Lanson NA Jr, Stallworth BS, Egeland DB, Delcarpio JB, Bahinski A, and Izzo NJ Jr (1998) HL-1 cells: a cardiac muscle cell line that contracts and retains phenotypic characteristics of the adult cardiomyocyte. *Proc Natl Acad Sci USA* **95:**2979–2984.
Cordes JS, Sun Z, Lloyd DB, Bradley JA, Opsahl AC, Tengowski MW, Chen X, and Zhou J (2005) Pentamidine reduces hERG expression to prolong the QT interval. *Br J Pharmacol* **145:**15–23.
de Boer TP, Nalos L, Stary A, Kok B, Houtman MJ, Antoons G, van Veen TA, Beekman JD, de Groot BL, Opthof T, et al. (2010) The anti-protozoal drug pentamidine blocks KIR2.x-mediated inward rectifier current by entering the cytoplasmic pore region of the channel. *Br J Pharmacol* **159:**1532–1541.
Dennis A, Wang L, Wan X, and Ficker E (2007) hERG channel trafficking: novel targets in drug-induced long QT syndrome. *Biochem Soc Trans* **35:**1060–1063.
Doyle DA, Morais Cabral J, Pfuetzner RA, Kuo A, Gulbis JM, Cohen SL, Chait BT, and MacKinnon R (1998) The structure of the potassium channel: molecular basis of K+ conduction and selectivity. *Science* **280:**69–77.
Fernandez D, Ghanta A, Kauffman GW, and Sanguinetti MC (2004) Physicochemical features of the HERG channel drug binding site. *J Biol Chem* **279:**10120–10127.
Fernandez D, Ghanta A, Kinard KI, and Sanguinetti MC (2005) Molecular mapping of a site for Cd^{2+}-induced modification of human ether-à-go-go-related gene (hERG) channel activation. *J Physiol* **567:**737–755.
Ficker E, Dennis A, Kuryshev Y, Wible BA, and Brown AM (2005) HERG channel trafficking. *Novartis Found Symp* **266:**57–69.
Ficker E, Dennis AT, Obejero-Paz CA, Castaldo P, Taglialatela M, and Brown AM (2000) Retention in the endoplasmic reticulum as a mechanism of dominant-negative current suppression in human long QT syndrome. *J Mol Cell Cardiol* **32:**2327–2337.
Ficker E, Dennis AT, Wang L, and Brown AM (2003) Role of the cytosolic chaperones Hsp70 and Hsp90 in maturation of the cardiac potassium channel HERG. *Circ Res* **92:**e87–100.
Ficker E, Jarolimek W, Kiehn J, Baumann A, and Brown AM (1998) Molecular determinants of dofetilide block of HERG K+ channels. *Circ Res* **82:**386–395.
Ficker E, Kuryshev YA, Dennis AT, Obejero-Paz C, Wang L, Hawryluk P, Wible BA, and Brown AM (2004) Mechanisms of arsenic-induced prolongation of cardiac repolarization. *Mol Pharmacol* **66:**33–44.
Ficker E, Obejero-Paz CA, Zhao S, and Brown AM (2002) The binding site for channel blockers that rescue misprocessed human long QT syndrome type 2 ether-a-gogo-related gene (HERG) mutations. *J Biol Chem* **277:**4989–4998.
Gang H and Zhang S (2006) Na+ permeation and block of hERG potassium channels. *J Gen Physiol* **128:**55–71.
***García-Ferreiro RE, Kerschensteiner D, Major F, Monje F, ***Stühmer W, and Pardo LA (2004) Mechanism of block of hEag1 K+ channels by imipramine and astemizole. *J Gen Physiol* **124:**301–317.
Girgis I, Gualberti J, Langan L, Malek S, Mustaciuolo V, Costantino T, and McGinn TG (1997) A prospective study of the effect of I.V. pentamidine therapy on ventricular arrhythmias and QTc prolongation in HIV-infected patients. *Chest* **112:** 646–653.
Gong Q, Keeney DR, Molinari M, and Zhou Z (2005) Degradation of trafficking-defective long QT syndrome type II mutant channels by the ubiquitin-proteasome pathway. *J Biol Chem* **280:**19419–19425.
Guo J, Li X, Shallow H, Xu J, Yang T, Massaeli H, Li W, Sun T, Pierce GN, and Zhang S (2011) Involvement of caveolin in probucol-induced reduction in hERG plasma-membrane expression. *Mol Pharmacol* **79:**806–813.
Guo J, Massaeli H, Xu J, Jia Z, Wigle JT, Mesaeli N, and Zhang S (2009) Extracellular K+ concentration controls cell surface density of IKr in rabbit hearts and of the HERG channel in human cell lines. *J Clin Invest* **119:**2745–2757.
Hishigaki H and Kuhara S (2011) hERGAPDbase: a database documenting hERG channel inhibitory potentials and APD-prolongation activities of chemical compounds. *Database* (*Oxford*) **2011:**bar017.
Kannankeril P, Roden DM, and Darbar D (2010) Drug-induced long QT syndrome. *Pharmacol Rev* **62:**760–781.
Kuryshev YA, Ficker E, Wang L, Hawryluk P, Dennis AT, Wible BA, Brown AM, Kang J, Chen XL, Sawamura K, et al. (2005) Pentamidine-induced long QT syndrome and block of hERG trafficking. *J Pharmacol Exp Ther* **312:**316–323.
Massaeli H, Guo J, Xu J, and Zhang S (2010) Extracellular K+ is a prerequisite for the function and plasma membrane stability of HERG channels. *Circ Res* **106:** 1072–1082.

Mitcheson JS, Chen J, Lin M, Culberson C, and Sanguinetti MC. (2000) A structural basis for drug-induced long QT syndrome. *Proc Natl Acad Sci USA* **97:**12329–12333.

Nacher M, Carme B, Sainte Marie D, Couppié P, Clyti E, Guibert P, and Pradinaud R (2001) Influence of clinical presentation on the efficacy of a short course of pentamidine in the treatment of cutaneous leishmaniasis in French Guiana. *Ann Trop Med Parasitol* **95:**331–336.

Obers S, Staudacher I, Ficker E, Dennis A, Koschny R, Erdal H, Bloehs R, Kisselbach J, Karle CA, Schweizer PA, et al. (2010) Multiple mechanisms of hERG liability: K+ current inhibition, disruption of protein trafficking, and apoptosis induced by amoxapine. *Naunyn Schmiedebergs Arch Pharmacol* **381:**385–400.

Ohnishi K, Yoshida H, Shigeno K, Nakamura S, Fujisawa S, Naito K, Shinjo K, Fujita Y, Matsui H, Sahara N, et al. (2002) Arsenic trioxide therapy for relapsed or refractory Japanese patients with acute promyelocytic leukemia: need for careful electrocardiogram monitoring. *Leukemia* **16:**617–622.

Ohnishi K, Yoshida H, Shigeno K, Nakamura S, Fujisawa S, Naito K, Shinjo K, Fujita Y, Matsui H, Takeshita A, et al. (2000) Prolongation of the QT interval and ventricular tachycardia in patients treated with arsenic trioxide for acute promyelocytic leukemia. *Ann Intern Med* **133:**881–885.

Pollard CE, Abi Gerges N, Bridgland-Taylor MH, Easter A, Hammond TG, and Valentin JP (2010) An introduction to QT interval prolongation and non-clinical approaches to assessing and reducing risk. *Br J Pharmacol* **159:**12–21.

Rajamani S, Eckhardt LL, Valdivia CR, Klemens CA, Gillman BM, Anderson CL, Holzem KM, Delisle BP, Anson BD, Makielski JC, et al. (2006) Drug-induced long QT syndrome: hERG K+ channel block and disruption of protein trafficking by fluoxetine and norfluoxetine. *Br J Pharmacol* **149:**481–489.

Sands M, Kron MA, and Brown RB (1985) Pentamidine: a review. *Rev Infect Dis* **7:**625–634.

Sanguinetti MC and Tristani-Firouzi M (2006) hERG potassium channels and cardiac arrhythmia. *Nature* **440:**463–469.

Soeiro MN, De Souza EM, Stephens CE, and Boykin DW (2005) Aromatic diamidines as antiparasitic agents. *Expert Opin Investig Drugs* **14:**957–972.

Staudacher I, Wang L, Wan X, Obers S, Wenzel W, Tristram F, Koschny R, Staudacher K, Kisselbach J, Koelsch P, et al. (2011) hERG K+ channel-associated cardiac effects of the antidepressant drug desipramine. *Naunyn Schmiedebergs Arch Pharmacol* **383:**119–139.

Takemasa H, Nagatomo T, Abe H, Kawakami K, Igarashi T, Tsurugi T, Kabashima N, Tamura M, Okazaki M, Delisle BP, et al. (2008) Coexistence of hERG current block and disruption of protein trafficking in ketoconazole-induced long QT syndrome. *Br J Pharmacol* **153:**439–447.

Thomsen MB, Matz J, Volders PG, and Vos MA (2006) Assessing the proarrhythmic potential of drugs: current status of models and surrogate parameters of torsades de pointes arrhythmias. *Pharmacol Ther* **112:**150–170.

van der Heyden MA, Smits ME, and Vos MA (2008) Drugs and trafficking of ion channels: a new pro-arrhythmic threat on the horizon? *Br J Pharmacol* **153:**406–409.

Wan X, Dennis AT, Obejero-Paz C, Overholt JL, Heredia-Moya J, Kirk KL, and Ficker E (2011) Oxidative inactivation of the lipid phosphatase phosphatase and tensin homolog on chromosome ten (PTEN) as a novel mechanism of acquired long QT syndrome. *J Biol Chem* **286:**2843–2852.

Wang L, Dennis AT, Trieu P, Charron F, Ethier N, Hebert TE, Wan X, and Ficker E (2009) Intracellular potassium stabilizes human ether-à-go-go-related gene channels for export from endoplasmic reticulum. *Mol Pharmacol* **75:**927–937.

Wang L, Wible BA, Wan X, and Ficker E (2007) Cardiac glycosides as novel inhibitors of human ether-a-go-go-related gene channel trafficking. *J Pharmacol Exp Ther* **320:**525–534.

Warmke JW and Ganetzky B (1994) A family of potassium channel genes related to eag in *Drosophila* and mammals. *Proc Natl Acad Sci USA* **91:**3438–3442.

Wharton JM, Demopulos PA, and Goldschlager N (1987) Torsade de pointes during administration of pentamidine isethionate. *Am J Med* **83:**571–576.

Wible BA, Hawryluk P, Ficker E, Kuryshev YA, Kirsch G, and Brown AM (2005) HERG-Lite: a novel comprehensive high-throughput screen for drug-induced hERG risk. *J Pharmacol Toxicol Methods* **52:**136–145.

Wu ZY, Yu DJ, Soong TW, Dawe GS, and Bian JS(2011) Progesterone impairs human ether-a-go-go-related gene (HERG) trafficking by disruption of intracellular cholesterol homeostasis. *J Biol Chem* **286:**22186–22194.

Zhang S (2006) Isolation and characterization of I(Kr) in cardiac myocytes by Cs+ permeation. *Am J Physiol Heart Circ Physiol* **290:**H1038–H1049.

Zou A, Xu QP, and Sanguinetti MC (1998) A mutation in the pore region of HERG K^+ channels expressed in *Xenopus* oocytes reduces rectification by shifting the voltage dependence of inactivation. *J Physiol* **509:**129–137.

Address correspondence to: Eckhard Ficker, Rammelkamp Center, MetroHealth Medical Center, 2500 MetroHealth Dr., Cleveland, OH 44109. E-mail: eficker@metrohealth.org